Nanoparticle as Signaling Protein Mimic: Robust Structural and Functional Modulation of CaMKII upon Specific Binding to Fullerene C60 Nanocrystals

Yanyan Miao,[†] Jing Xu,[†] Yi Shen, Liang Chen, Yunpeng Bian, Yi Hu, Wei Zhou, Fang Zheng, Na Man, Yuanyuan Shen, Yunjiao Zhang, Ming Wang,* and Longping Wen*

Hefei National Laboratory for Physical Sciences at Microscale and School of Life Sciences, University of Science & Technology of China, Hefei, Anhui 230027, China. [†]Y. Miao and J. Xu contributed equally to this work.

ABSTRACT In a biological environment, nanoparticles encounter and interact with thousands of proteins, forming a protein corona on the surface of the nanoparticles, but these interactions are oftentimes perceived as nonspecific protein adsorption, with protein unfolding and deactivation as the most likely consequences. The potential of a nanoparticle—protein interaction to mimic a protein—protein interaction in a cellular signaling process, characterized by stringent binding specificity and robust functional modulation for the interacting protein, has not been adequately demonstrated. Here, we show that water-suspended fullerene C60 nanocrystals (nano-C60) interact with and modulate the function of the Ca^{2+}/calmodulin-dependent protein kinase II (CaMKII), a multimeric intracellular serine/threonine kinase central to Ca^{2+} signal transduction, in a fashion that rivals the well-documented interaction between the NMDA (*N*-methyl-D-aspartate) receptor subunit NR2B protein and CaMKII. The stable high-affinity binding of CaMKII to distinct sites on nano-C60, mediated by amino acid residues D246 and K250 within the catalytic domain of CaMKIIα, but not the nonspecific adsorption of CaMKII to diamond nanoparticles, leads to functional consequences reminiscent of the NR2B—CaMKII interaction, including generation of autonomous CaMKII activity after Ca^{2+} withdrawal, calmodulin trapping and CaMKII translocation to postsynaptic sites. Our results underscore the critical importance of specific interactions between nanoparticles and cellular signaling proteins, and the ability of nano-C60 to sustain the autonomous kinase activity of CaMKII may have significant implications for both the biosafety and the potential therapeutic applications of fullerene C60.

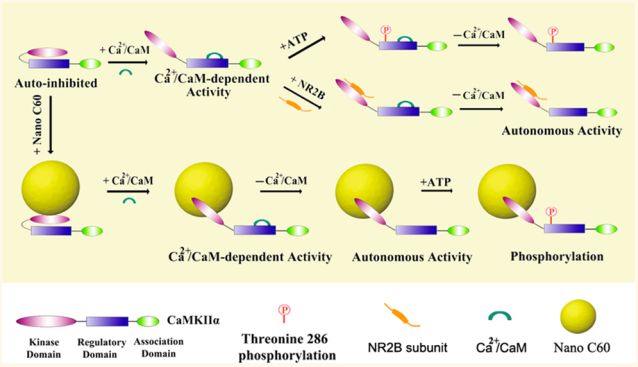

KEYWORDS: fullerene C60 nanocrystals · Ca^{2+}/CaM-dependent protein kinase II · NMDA receptor subunit NR2B protein · specific interaction · amino acid residues · T286 autophosphorylation · autonomous activity

Nanoparticle—protein interactions hold one of the keys for understanding the diverse and oftentimes unexpected biological effects elicited by engineered nanomaterials.[1−4] In a biological environment such as in the blood circulation, intercellular space within tissues or inside a cell, nanoparticles may encounter and interact with thousands of proteins. Some of these interactions may be transient, with proteins on a come-and-go basis, while others are stable, with proteins getting "adsorbed" and forming a protein conora on the surface of nanoparticles.[3,5,6] The physicochemical properties of the nanoparticles are likely to exert an influence on an interacting protein's structure and function, possibly leading to manifestation of biological effects. Indeed, conformational loss and alterations are commonly observed for proteins bound to inorganic nanoparticles,[7−9] which typically display hydrophobic surfaces. As a result, protein denaturation[10] and inactivation[11,12] have frequently been reported for proteins bound to

* Address correspondence to lpwen@ustc.edu.cn, wming@ustc.edu.cn.

Received for review March 17, 2014 and accepted May 26, 2014.

Published online May 26, 2014
10.1021/nn501495a

inorganic nanoparticles, with the resulting biological consequences such as inflammation.[13] In certain situations, an interacting nanoparticle may positively modify a protein's functionality, such as exposing cryptic epitope,[6,14] forming novel protein assemblies,[7,15] or enhancing the protein's enzymatic activity.[16−18] However, despite the considerable amount of work that has been done, our current understanding on protein−nanoparticle interactions, particularly with the view from the protein side, is still rather limited. Many of the published studies have treated the stable association of proteins to nanoparticles as nonspecific "adsorption", but in almost all of the cases where the binding mechanism has been determined, sequence-specific and conformationally driven interactions were uncovered.[8,19] Moreover, few studies have carefully addressed the potential impact of a nanoparticle interaction on the functionality of important cellular proteins in physiological settings. Take a lesson from the extensively studied protein−protein interactions found in many cellular signaling pathways. In these processes, signals for driving critically important cell decisions such as growth or differentiation are oftentimes transmitted through the highly specific interaction between two protein molecules, causing changes in the functionality for one or both of the proteins, such as the protein's enzymatic activity, intracellular location, or association with other signaling proteins. Nanoparticles, with many characteristics similar to proteins,[20−23] could conceivably act like a signaling protein in transmitting signals through interacting with appropriate protein partners, but this has not been adequately shown.

Buckminster fullerene C60 (C60) is a classic engineered nanomaterial with a remarkable geometrical structure and unique physicochemical properties.[24,25] C60 and its derivatives are currently being actively pursued as potential therapeutic agents for many human diseases owing to their outstanding biological activities, including antibacteria, antiviral, autophagy induction, apoptosis modulation, ion channel blockage, neuroprotection and so on.[26−30] Some of these effects are likely manifested through C60 interaction with the key proteins involved in the underlying biological processes. Indeed, more than 20 proteins are known to stably bind to C60 or its derivatives,[31] and many more proteins are predicted to interact with C60,[31] even though direct proof for interaction-resulted functional modulation has been obtained for only a few of the proteins.

In this report we revealed a stable high-affinity interaction between the Ca^{2+}/calmodulin (CaM)-dependent protein kinase II (CaMKII), a multimeric intracellular serine/threonine kinase central to Ca^{2+} signal transduction, and the water-suspended C60 nanocrystals (nano-C60). This highly specific interaction, dictated by distinct sites on the nanocrystal surface and a set of amino acids within the catalytic domain of the CaMKIIα subunit, is reminiscent of the well-documented interaction between CaMKII and the NMDA receptor subunit NR2B, a neuronal membrane protein that also binds to the catalytic domain of CaMKII.[32] Analogous to NR2B−CaMKII interaction, binding of CaMKII to nano-C60 locks CaMKII in an active conformation, leading to generation of autonomous CaMKII activity in the absence of T286 autophosphorylation, calmodulin (CaM) trapping and translocation to postsynaptic sites for CaMKII. Our results provide a compelling example that an inorganic nanoparticle has the capacity to act like a cellular signaling protein in exerting robust structural and functional modulation for an interacting protein.

RESULTS

Stable and High-Affinity Interaction between CaMKIIα and Nano-C60. A previous report that C60 derivatives may exert neuroprotective functions by blocking glutamate receptors[29] prompted us to search for potential high affinity C60-interacting proteins in the brain. Nano-C60 were prepared by the standard THF evaporation procedure and exhibited an average size of 120 nm, as visualized by transmission electron microscopy (TEM) (Supporting Information Figure S1). We incubated nano-C60 with rat brain protein extract in the presence of excess bovine serum albumin, a known C60-binding protein, then precipitated nano-C60 and any interacting proteins by centrifugation after extensive washing. A large number of proteins remained bound to nano-C60 (Supporting Information Figure S2). We focused on band 1 around 54 kd, as it exhibited dramatic enrichment in the nano-C60 precipitate as compared to the extract. Mass spectrometry (MS) analysis identified several protein candidates for band 1 (Supporting Information Table S1), with the α subunit of CaMKII (CaMKIIα) as the most likely one. Western blotting verified the CaMKIIα identity (Figure 1A). Western blotting also revealed the presence of the β subunit of CaMKII (CaMKIIβ) in the nano-C60 precipitate (Figure 1A). Consistent with this, CaMKIIβ was one of the protein species identified by MS in the SDS gel position where CaMKIIβ migrated (band 2 in Supporting Information Figure S2; MS data shown in Supporting Information Table S2), even though no discrete protein band was observed in that position. In contrast, glyceraldehyde 3-phosphate dehydrogenase (GAPDH), a control cytoplasmic protein, did not precipitate with nano-C60, indicating that the interaction of nano-C60 with CaMKII had protein specificity. Binding of CaMKII to nano-C60 also exhibited nanomaterial selectivity, as single-walled carbon nanotubes precipitated small amount of GAPDH and no CaMKII, while nanodiamond precipitated small amount of CaMKII and large amount of GAPDH, under the same experimental conditions (Figure 1B). To assess which subunit, or both, of CaMKII binds directly to nano-C60, we expressed CaMKIIα and CaMKIIβ separately in COS-7 cells, a cell line that showed very little endogenous expression of either subunit

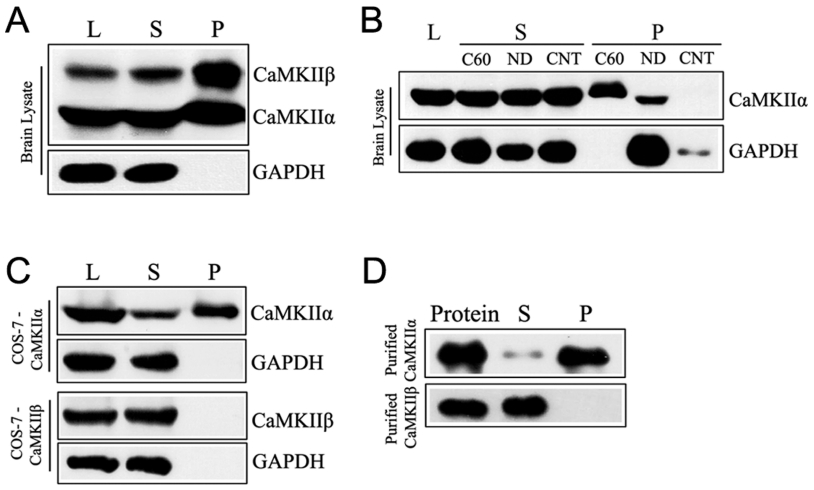

Figure 1. Identification of CaMKIIα as a major nano-C60-interacting protein in the brain extract. (A) Rat forebrain lysate (200 μL, containing 1.2 mg protein) was incubated with 1.2 μg of nano-C60 in a standard binding assay. Proteins were separated on an SDS gel followed by Western blotting. (B) Rat forebrain lysate was precipitated with 1.2 μg of nano-C60 (C60), nanodiamond (ND) or carbon nanotube (CNT) and then analyzed by Western blotting with CaMKIIα and GAPDH antibody, respectively. (C) Lysates (50 μL) from COS-7 cells transfected with CaMKIIα (upper panel) or CaMKIIβ (lower panel) were precipitated by 0.4 μg of nano-C60 and analyzed by Western blotting. (D) 5 μg of purified CaMKIIα and CaMKIIβ were individually precipitated with 0.4 μg of nano-C60 and then analyzed by Western blotting with their respective antibodies. For (A−D), L is the lysate before precipitation, while S and P are the supernatant and the pellet, respectively, derived from the precipitation.

(Supporting Information Figure S3). Nano-C60 precipitated CaMKIIα, but not CaMKIIβ, from these cell extracts (Figure 1C). Using purified proteins, we further confirmed that nano-C60 precipitated CaMKIIα but not CaMKIIβ (Figure 1D). These results established that nano-C60 interacts directly with CaMKIIα but not CaMKIIβ, and CaMKIIβ in the hippocampal extract was pulled down by nano-C60 due to the association of CaMKIIβ with CaMKIIα, as it is known that most of the CaMKII in the hippocampus exist as a dodecameric protein complex composed of 9 α and 3 β subunits.[33]

A protein corona on the surface of the nanoparticles would be expected to form when nano-C60 enters a cell or bloodstream, and the protein corona might affect the interaction between nano-C60 and CaMKIIα. We thus assessed the ability of nano-C60 to bind CaMKIIα after preincubating the nanoparticles with fetal bovine serum (FBS) or COS-7 cell lysate. Multiple proteins from either FBS or COS-7 lysate were precipitated by nano-C60, indicative of the protein corona formation (Supporting Information Figure S4, A and B), but they did not affect the subsequent binding of CaMKIIα to nano-C60 (Supporting Information Figure S4, C and D). To further assess the relative binding strength between nano-C60 and CaMKIIα, we performed nano-C60 precipitation of the purified CaMKIIα in the presence of excess bovine serum albumin (BSA), a protein that has been shown to interact with prestine C60.[31] Up to 250 μg/mL of BSA, representing 50 fold over the concentration of CaMKIIα, had no effect on the amount of CaMKIIα precipitated by nano-C60 (Supporting Information Figure S5). No BSA was detected in the precipitate under these conditions. However, in the absence of other proteins, a small amount of pure BSA did bind to nano-C60 and became precipitated (Supporting Information Figure S6). These results indicated that the relatively weak binding between nano-C60 and BSA was competed out by CaMKIIα. CaMKIIα binds to nano-C60 rapidly, with the maximum amount of bound CaMKIIα achieved within 1 min after the addition of nano-C60 to the hippocampal extract (Figure 2A). Binding of pure CaMKIIα to nano-C60 was also dose-dependent, as the amount of precipitated CaMKIIα increased, and the amount of CaMKIIα remaining in the supernatant decreased, with the increasing dose of nano-C60 (Figure 2B). 1.6 μg of nano-C60 was sufficient to completely precipitate 1.5 μg of CaMKIIα as shown by Western blotting. This gave rise to a binding capacity of 0.94 μg, or 0.017 nmol, of CaMKIIα per μg of nano-C60. Given a density of 1.56×10^9 nanoparticles per μg of nano-C60 as revealed by Nanoparticle Tracking Analysis, we estimated that up to 6686 CaMKIIα protein molecules can be bound onto one nano-C60 particle, which exhibited an average diameter of 120 nm (Supporting Information Figure S7A). This compared to the reported 7 fibrinogen protein molecules bound to each poly(acrylic acid)-coated gold nanoparticle with the size of 20 nm.[13] A different assay using enzyme-linked immunosorbent assay (ELISA) revealed a somewhat larger but comparable binding capacity of 3.64 μg of CaMKIIα per μg of nano-C60 (Supporting Information Figure S8). Both nano-C60 (zeta potential −13.5 mV) and CaMKIIα (PI = 6.6) exhibited a negative charge under the above binding conditions, and the nano-C60−CaMKIIα complex (zeta potential −30 mV) was even more negatively charged (Supporting Information Figure S7B). The interaction of nano-C60 with CaMKIIα did not require, nor was affected by, photoactivation

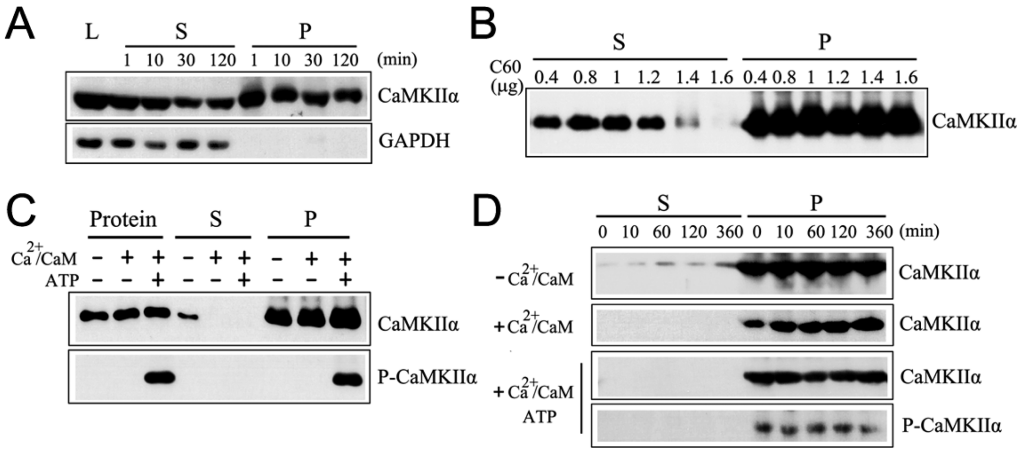

Figure 2. Stable and high-affinity interaction between nano-C60 and CaMKIIα. (A) Time course of nano-C60 binding to CaMKIIα. Rat forebrain lysate was subject to binding assay with nano-C60 for the indicated times and then analyzed with CaMKIIα and GAPDH antibody, respectively. (B) Purified CaMKIIα (1.5 μg) was assayed for binding to the increasing amounts of nano-C60 and analyzed by Western blotting with CaMKIIα antibody. (C) Effect of Ca^{2+}/CaM activation (500 μM Ca^{2+} plus 1 μM calmodulin) and autophosphorylation (1 mM ATP) on the binding of partially purified forebrain CaMKIIα to nano-C60. (D) Time course of dissociation of bound rat forebrain CaMKIIα from nano-C60, detected by Western blotting with CaMKIIα antibody. Effect of Ca^{2+}/CaM activation and autophosphorylation on this dissociation is also shown. Autophosphorylation was verified by the phosphor-specific antibody (P-CaMKII) against CaMKIIα. For (A−D), L is the lysate before precipitation, while S and P are the supernatant and the pellet, respectively, derived from the precipitation.

(Supporting Information Figure S9). Glutathione (GSH), a free radical scavenger, had no effect on nano-C60−CaMKII interaction (data not shown). These results indicated that binding of CaMKIIα to nano-C60 does not involve free radicals.

CaMKII is a multimeric protein typically composed of 12 subunits. Each subunit contains three key domains: a catalytic domain for performing the kinase function, a regulatory domain for modulating the enzyme activation, and an association domain for directing multimeric assembly.[33] Under resting conditions, the regulatory domain interacts with the N-terminal catalytic domain, blocking substrate binding and rendering the kinase autoinhibited, while binding of Ca^{2+}/CaM to the regulatory domain elicits a conformational shift that relieves autoinhibition and activates the kinase. In the lengthy presence of Ca^{2+}/CaM, CaMKII undergoes intersubunit autophosphorylation at T286 (T286 for CaMKIIα, T287 for CaMKIIβ) within the CaMKII autoinhibitory region, preventing interaction between the kinase domain and the autoinhibitory region and resulting in Ca^{2+}/CaM-independent activity. While basal-state CaMKII did bind to nano-C60, kinase activation by Ca^{2+}/CaM increased the amount of CaMKII precipitated by nano-C60, and autophosphorylation by ATP further enhanced nano-C60−CaMKII interaction (Figure 2C). A previous study by Cedervall *et al.* found a large variation in dissociation rates for proteins bound on nanoparticles.[5] To assess the stability of the interaction between CaMKIIα and nano-C60, we incubated the nano-C60 precipitate of CaMKIIα in saline and monitored the release of bound CaMKIIα at the various time points by Western blotting. Only a small amount (about 8.6%) of basal-state CaMKIIα was found to dissociate from nano-C60 over a period of 6 h (Figure 2D), indicating that binding of CaMKIIα to nano-C60 was highly stable. Treatment of the precipitate with Ca^{2+}/CaM, and subsequently with ATP, resulted in even less (<3%) release of CaMKIIα from nano-C60, consistent with the binding studies showing that the activated CaMKII exhibited higher affinity toward nano-C60.

Indentification of the Nano-C60 Binding Sites on CaMKIIα. To map the region of CaMKIIα responsible for nano-C60 binding, we expressed in *E. coli* three fragments of CaMKIIα: α1 (amino acids 1−273, containing the catalytic domain), α2 (amino acids 274−478, containing the regulatory domain plus the association domain), and α3 (amino acids 313−478, containing the association domain only) (Figure 3A). High-affinity binding to nano-C60 was observed for the purified α1 fragment, but not the α2 and α3 fragments (Figure 3B). The full-length CaMKIIα and the α1 fragment exhibited similar high binding affinity toward nano-C60 (Figure 3C). Addition of excess amount of purified α1 fragment to rat hippocampal lysate decreased the amount of CaMKIIα precipitated by nano-C60, but had minimal effect on the precipitation of other proteins (Supporting Information Figure S10). This result, together with the data showing that the preformed protein corona from FBS or COS-7 lysate did not affect the binding of CaMKIIα to nano-C60 (Supporting Information Figure S4), strongly suggested the presence of distinct sites on nano-C60 that selectively bind CaMKIIα.

To further locate the binding site on the protein, we took advantage of the fact that CaMKIIα, but not CaMKIIβ, binds to nano-C60. A comparison of the sequence between the catalytic domains of the two

subunits revealed differences in 24 amino acid residues (Supporting Information Figure S11). We made point mutations on residues exhibiting nonconserving changes between the two subunits, converting the residues in CaMKIIα to the corresponding ones found in CaMKIIβ. While most of the single amino acid changes did not significantly alter CaMKIIα binding to nano-C60 (with H84F and P189A as two examples), two of the point mutants (D246N and K250Q) exhibited dramatic decrease in binding to nano-C60 (Figure 4A). The double mutant CaMKIIα (D246N/K250Q) completely lost the ability to bind to nano-C60, but had no effect on binding to nanodiamond (Figure 4B). These results indicate that CaMKIIα binds to nano-C60 and nanodiamond *via* different mechanisms. On the basis of the published crystal structure of CaMKII holoenzyme,[34] D246 and K250 are located on the helix 6 of the CaMKIIα molecule and are exposed on the surface of the holoenzyme, thus most likely accessible for nano-C60 binding (Supporting Information Figure S12). Collectively, the above results demonstrated a stable, high-affinity interaction between distinct sites on nano-C60 and specific residues on the catalytic domain of CaMKIIα, an interaction that is further strengthened by the activation of the kinase function for the CaMKII holoenzyme. In comparison, NR2B also binds specifically to the catalytic domain of CaMKII, involving a set of amino acid residues including isoleucine 205 (I205) and tryptophan 237 (W237), but unlike nano-C60, NR2B binds only to preactivated CaMKII.[35]

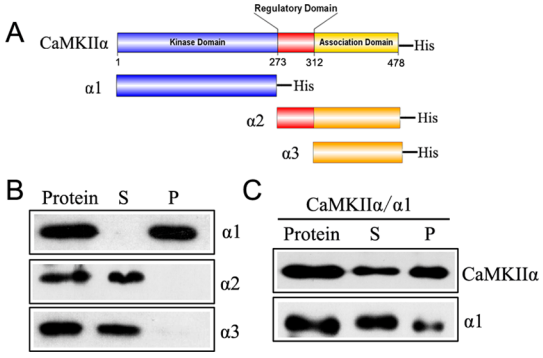

Figure 3. Mapping nano-C60-binding domain of CaMKIIα. (A) Diagram of CaMKIIα protein and the three protein fragments produced in *E. coli*, all with His-tag at the C-terminus. (B) 1.5 μg of purified α1, α2 and α3 were assayed for binding to 0.4 μg of nano-C60 and then analyzed by Western blotting with the His-tag antibody. (C) A mixture of 1.5 μg each of CaMKIIα and α1 was subject to binding assay with 0.4 μg of nano-C60 and then analyzed by Western blotting with His-tag antibody. For (B) and (C), S and P are the supernatant and the pellet, respectively, derived from the precipitation.

Binding to Nano-C60 Elicits CaMKIIα Autonomous Activity. Binding of CaMKII to NR2B has been shown to elicit autonomous activity for CaMKII.[32] To assess the potential impact of nano-C60 binding on CaMKII protein function *in vitro*, we conducted kinase assays using the CaMKII holoenzyme partially purified from rat hippocampus and measuring the phosphorylation of the substrate syntide-2 with ^{32}P-ATP. Consistent with the reported results, the basal CaMKII's enzymatic activity was minimal but exhibited an 11-fold increase after Ca^{2+}/CaM stimulation, and this stimulated activity was largely abolished after the quenching of Ca^{2+} by EGTA (Figure 5A). Nano-C60 did not affect the basal CaMKII activity, but sustained the Ca^{2+}/CaM-stimulated CaMKII activity after the removal of Ca^{2+} by EGTA, analogous to the effect of T286 autophosphorylation by ATP or binding with NR2B. A different assay, using proteins expressed in COS-7 cells and a nonradioactive approach, revealed that nano-C60 sustained the Ca^{2+}/CaM-autonomous activity for the wild-type but not the double mutant (D246N/K250Q) CaMKIIα, demonstrating that binding to nano-C60 is critical for sustaining Ca^{2+}/CaM-autonomous activity (Figure 5B). The T286A mutant of CaMKIIα, which exhibited normal binding to nano-C60 (data not shown), also showed sustained Ca^{2+}/CaM-autonomous activity upon interacting with nano-C60, indicating that the threonine

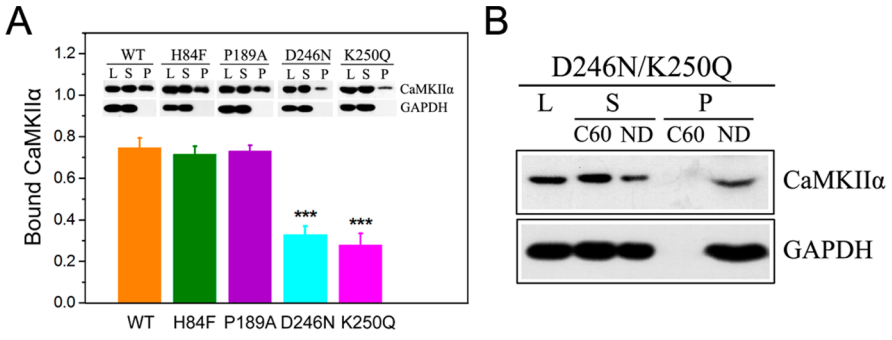

Figure 4. Identification the nano-C60 binding sites of CaMKIIα. (A) Lysate (50 μL) from COS-7 cells transfected with wild type (WT), H84F, P189A, D246N or K250Q CaMKIIα was precipitated by 0.4 μg of nano-C60 and analyzed by Western blotting with CaMKIIα and GAPDH antibody. The statistical graph showed the level of CaMKIIα in the pellet relative to that in the lysates, Mean ± SEM, n = 3, ***P < 0.005 *versus* wild type (WT). (B) COS-7 cell lysate (50 μL) transfected with D246N/K250Q double mutant CaMKIIα was precipitated with 0.4 μg of nano-C60 (C60) or nanodiamond (ND) and then analyzed by Western blotting with CaMKIIα and GAPDH antibody, respectively. For (A) and (B), L is the lysate before precipitation, while S and P are the supernatant and the pellet, respectively, derived from the precipitation.

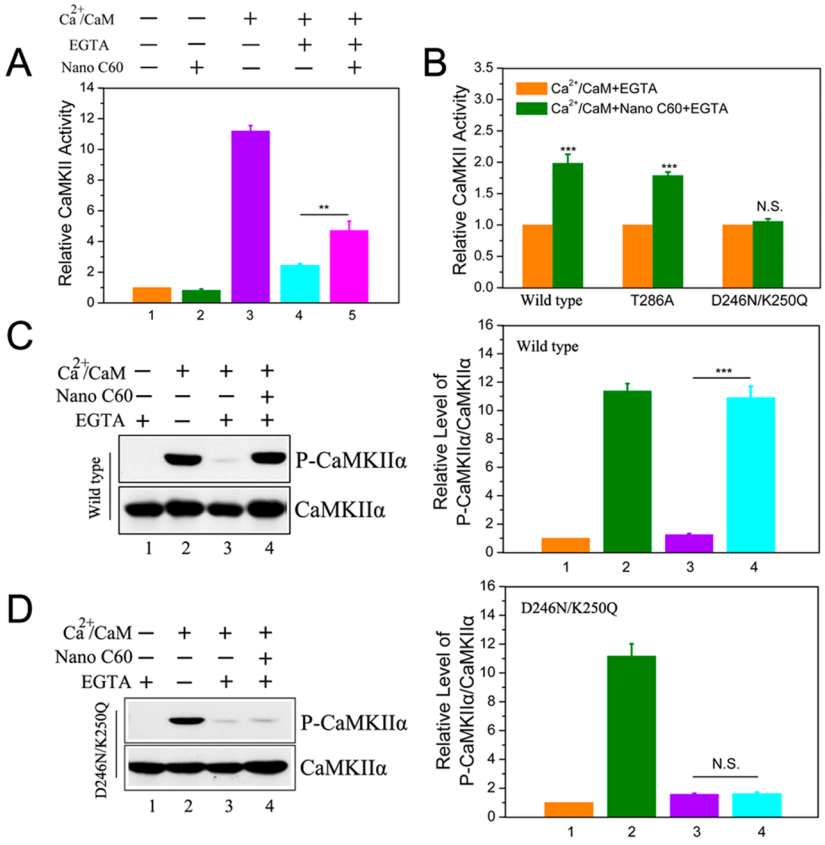

Figure 5. Generation autonomous kinase activity of CaMKII by binding to nano-C60 *in vitro*. (A) Radioactive kinase assays for the partially purified rat forebrain CaMKII, with syntide-2 as the substrate. The activity produced by the basal-state CaMKII (without Ca^{2+}/CaM and without nano-C60) was set at 1 and used to normalize the relative activity for other treatments. Mean ± SEM, $n = 5$, $^{**}P < 0.01$. (B) Nonradioactive assays for Ca^{2+}/CaM-independent activity of wild type CaMKIIα and two of its mutants expressed in COS-7 cells, using syntide-2 as the substrate. The kinase activity generated by the control treatment (without nano-C60) was set at 1 and used to normalize the relative activity for nano-C60 treatment. Mean ± SEM, $n = 3$, $^{***}P < 0.005$, N.S.: $p > 0.05$. (C,D) T286 autophosphorylation assay for the wild type (C) and D246N/K250Q double mutant CaMKIIα (D) produced in COS-7 cells, detected by CaMKII and antiphospho CaMKII antibodies. The right panel in (C) and (D) showed the level of P-CaMKIIα relative to that of CaMKIIα, with the value for control (without Ca^{2+}/CaM and without nano-C60) set at 1. Mean ± SEM, $n = 3$, $^{***}P < 0.005$, N.S.: $p > 0.05$.

286 residue, and T286 autophosphorylation, is not required for nano-C60 to modulate CaMKIIα's kinase activity. A third *in vitro* assay, the T286 autophosphorylation of CaMKIIα expressed in COS-7 cells, further confirmed nano-C60s ability to elicit Ca^{2+}/CaM-autonomous kinase activity through specifically binding to the protein (Figure 5, C and D), while nanodiamond, which also binds CaMKIIα but *via* a different mechanism, and fullerenol, a soluble fullerene derivative, did not possess this capability (Supporting Information Figure S13). In agreement with the substrate-based assay, Ca^{2+}/CaM-independent T286 autophosphorylation of CaMKIIα elicited by nano-C60 required Ca^{2+}/CaM preactivation (Supporting Information Figure S14). Moreover, Ca^{2+}/CaM-independent T286 autophosphorylation only occurred for nano-C60-bound CaMKIIα but not for CaMKIIα remaining in the supernatant after nano-C60 precipitation (Supporting Information Figure S15), again demonstrating that binding to nano-C60 is a prerequisite for generating Ca^{2+}/CaM-autonomous kinase activity of CaMKII. Collectively, these results provided comprehensive proof that nano-C60, similar to NR2B, has the ability to elicit Ca^{2+}/CaM-autonomous kinase activity on the bound CaMKII protein, with a prerequisite for Ca^{2+}/CaM prestimulation.

Binding of CaMKIIα to Nano-C60 Induces CaM Trapping. Another effect elicited by NR2B−CaMKII interaction, and also by T286 autophosphorylation of CaMKII, is CaM trapping, which refers to a striking >1000-fold increase in CaMKII's affinity toward CaM,[36] We thus assessed whether CaMKII−nano-C60 interaction has the same capability. Indeed, release of preloaded, nano-C60-treated CaMKIIα from Calmodulin Sepharose upon the addition of excess CaM was greatly reduced compared to the release of CaMKIIα without nano-C60 treatment (Figure 6A), indicative of CaM trapping for nano-C60-bound CaMKIIα. A different assay, based on the finding that Rhodamine-Calmodulin (R-CaM) bound to CaMKIIα exhibited much greater fluorescence than R-CaM in solution,[36−38] also revealed higher affinity of CaM on CaMKII after nano-C60 treatment (Figure 6B). As would be expected,

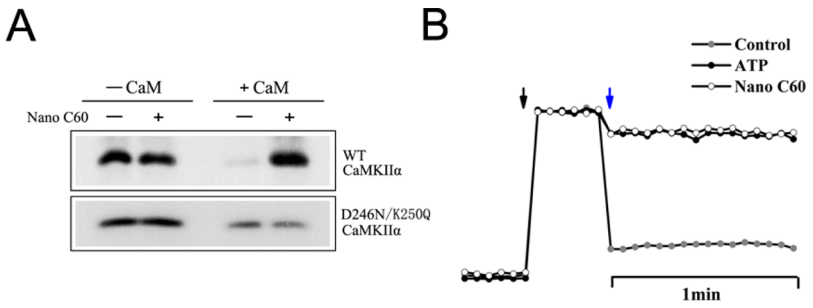

Figure 6. CaM trapping elicited by nano-C60. (A) COS-7-expressed wild type or D246N/K250Q double mutant CaMKIIα was loaded to the affinity column and then treated with or without nano-C60. CaM trapping as revealed by the amount of CaMKIIα, preloaded to Calmodulin Sepharose, remaining in the sepharose after elution with an excess CaM. (B) The fluorescence intensity of R-CaM in the mixture with partially purified rat hippocampal CaMKII, Ca^{2+}, unlabeled CaM, H_2O or ATP or nano-C60. CaMKII protein was added into the buffer with Ca^{2+} and R-CaM (black arrow), followed by treatment with H_2O, ATP or nano-C60. Release of R-CaM (25 nM) was initiated after addition of 300-fold excess of unlabeled CaM (7.5 μM) (blue arrow).

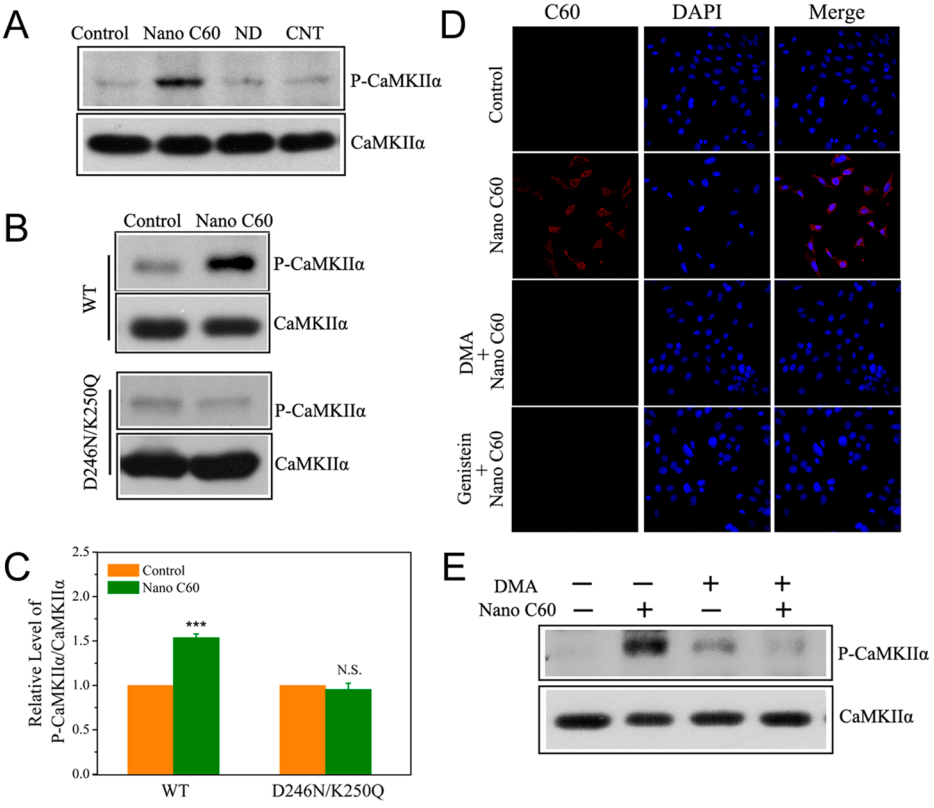

Figure 7. Generation of autonomous CaMKII kinase activity in cells by nano-C60. (A) HT22 hippocampal neuronal cells were treated with nano-C60, nanodiamond or CNT for 1 h. The level of CaMKII autophosphorylation at T286 was analyzed by immunoblotting using antibodies against CaMKII and phospho-CaMKII. (B) CaMKII autonomous activity for the wild type (WT) and D246N/K250Q double mutant CaMKIIα in COS-7 cells after nano-C60 treatment was detected by antibodies against CaMKII and phospho-CaMKII. (C) The panel showed the level of P-CaMKIIα in (B) relative to that of CaMKIIα, with the value for control (without nano-C60) set at 1. Mean ± SEM, $n = 3$, $^{***}P < 0.005$. In (D) and (E) HT22 cells were pretreated without or with the indicated endocytosis inhibitors (genistein and DMA) before nano-C60 addition. (D) Immunofluorescence was performed with antibody against C60, with nuclei staining with hoechst. The internalized nano-C60 was observed by fluorescent microscopy. (E) The CaMKIIα activity was detected by Western blotting with antibodies against CaMKII and phospho-CaMKII.

T286 autophosphorylation of CaMKII by ATP had the same reducing effect on CaM release. These results indicated that binding of CaMKII to nano-C60, similar to binding of CaMKII to NR2B, induced CaM trapping.

Nano-C60 Internalized into Cells Elicits CaMKIIα Autonomous Activity. Addition of nano-C60, but not that of nanodiamond or CNT, to the culture medium elicited persistent activation of CaMKIIα in HT22 hippocampal neuronal cells (Figure 7A). Furthermore, nano-C60 added to the culture medium caused persistent activation of the wild-type, but not the D246N/K250Q double mutant, CaMKIIα in COS-7 cells that expressed these proteins (Figure 7, B and C), consistent with the *in vitro* studies showing that the ability to bind to nano-C60 is a

prerequisite for sustained CaMKIIα activation. These results also suggested that nano-C60 could effectively enter cells to interact with CaMKIIα, a cytosolic protein. Indeed, the presence of nano-C60 in the cytoplasm was confirmed by fluorescent microscopy in cultured HT22 hippocampal neuronal cells using specific antibody against fullerene C60 (Figure 7D). The endocytosis inhibitors genistein[39] and dimethyl amiloride (DMA)[40] effectively reduced nano-C60 internalization, indicating that endocytosis was an important pathway for cellular uptake of nano-C60. The two inhibitors also abolished the ability of nano-C60 to elicit persistent activation of cellular CaMKIIα (Figure 7E and Supporting Information Figure S16, respectively), consistent with the notion that cellular internalization is essential for nano-C60 to interact with activate CaMKIIα.

Binding to Nano-C60 Induces Postsynpatic CaMKIIα Translocation. NR2B−CaMKII interaction, or CaMKII T286 autophosphorylation, can elicite CaMKIIα translocation to postsynaptic sites.[32,41] We thus assessed whether nano-C60 elicits the same effect on translocation of GFP-tagged CaMKIIα (GFP-CaMKIIα) in cultured neurons (Figure 8). In the untreated cells, both the wild-type and the D246N/K250Q double mutant GFP-CaMKIIα were distributed uniformly throughout dendritic shafts. However, after stimulation with 50 μM glutamate for 5 min, both forms of GFP-CaMKIIα exhibited enrichment in punctuate structures along dendritic processes. Nano-C60 treatment for 25 min caused similar enrichment in punctuate structures for the wild-type but not the double mutant GFP-CaMKIIα, while nanodiamond treatment caused no such enrichment for either the wild-type or the double mutant protein. Thus, analogous to NR2B interaction, specific binding to nano-C60 leads to postsynaptic translocation of CaMKIIα. The functional implication of this nano-C60-elicited translocation remains to be determined.

Binding to Nano-C60 Locks CaMKIIα in an Active Conformation. To further probe the activation mechanism, we employed Camuiα, a fluorescence resonance energy transfer (FRET) probe molecule of CaMKIIα.[42] Activation of COS-7-expressed Camuiα by Ca^{2+}/CaM resulted in an increase in the relative CFP/YFP ratio, indicative of the conformational change caused by the release of the autoinhibitory domain, but upon quenching of Ca^{2+} by EGTA, the relative CFP/YFP ratio decreased to the preactivation level, indicative of the reassociation of the autoinhibitory domain with the catalytic domain (Figure 9A). In contrast, Camuiα bound to nano-C60 showed normal CFP/YFP ratio increase upon Ca^{2+}/CaM activation but little decrease upon EGTA quenching, strongly suggesting that the reassociation of the autoinhibitory domain with the catalytic domain was inhibited. Consistent with the kinase activity data, Camuiα bound to nanodiamond exhibited the same FRET changes as the unbound Camuiα both before and after EGTA quenching, confirming that nanodiamond

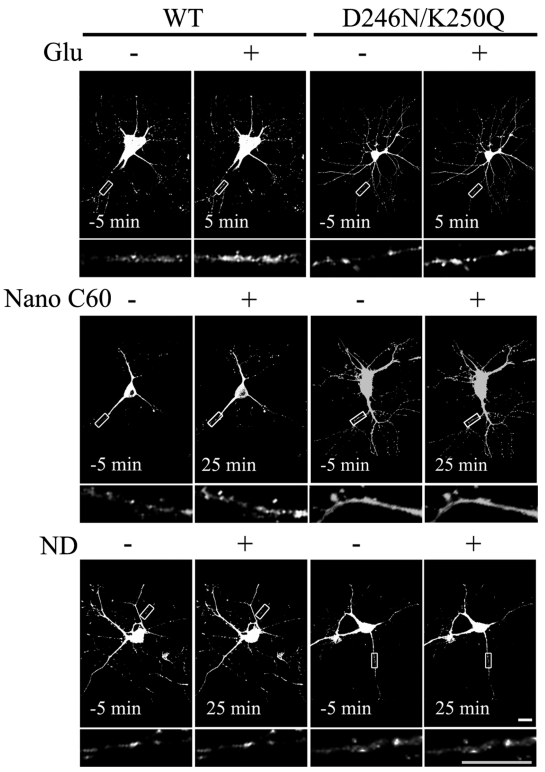

Figure 8. CaMKIIα translocation induced by nano-C60. Primary neurons transfected with wild-type (WT) or D246N/K250Q double mutant GFP-CaMKIIα were treated with 50 μM glutamate, 0.2 μg/mL of nano-C60 and nanodiamond (ND), respectively. The translocation of GFP-CaMKIIα was observed with an excitation wavelength at 488 nm. Scale bar indicated 10 μm (upper) or 2 μm (bottom).

was unable to lock CaMKIIα in the active conformation. This conformation-locking effect of nano-C60 was observed for Ca^{2+}/CaM preactivated wild-type but not the D246N/K250Q double mutant (Figure 9, B and C), demonstrating the critical importance of nano-C60 binding.

To visualize CaMKII activation by nano-C60 in live cells, we expressed Camuiα in cultured hippocampal neurons and observed cells by confocal microscopy. After CFP-specific excitation, we detected signals in both CFP and YFP channels (Supporting Information Figure S17A). After photobleaching of YFP, we observed a dequenching of the CFP signal, confirming FRET in neurons (Supporting Information Figure S17B). Addition of nano-C60 to the culture medium led to gradual activation of the wild-type Camuiα in dendrites, as revealed by the increased CFP/YFP ratio, with maximum activation achieved at about 40 min (Figure 9D). In agreement with the solution assay results (Figure 9C), nano-C60 did not activate the D246N/K250Q Camuiα double mutant, nor did nanodiamond activate the wild-type Camuiα, in dendrites. As a control, stimulation with 50 μM glutamate led to a rapid activation in dendrites for both the wild-type and the double mutant Camuiα, with the FRET response returned to the basal level after washout (Supporting Information Figure S18).

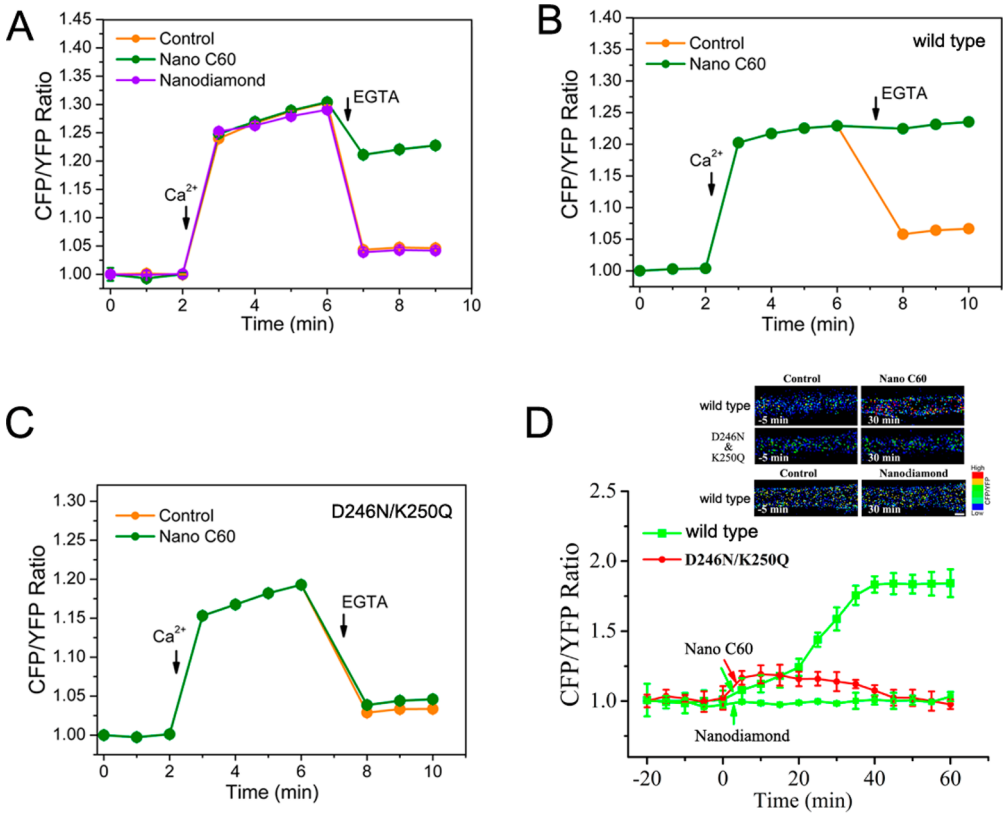

Figure 9. Conformational change of CaMKIIα caused by binding to nano-C60. (A) FRET response of Camuiα expressed in 293T cells that was in the lysate (Control), bound to nano-C60, or bound to nanodiamond. Ca^{2+} and EGTA were added as indicated. (B,C) Emission fluorescence spectra of wild type (B) or D246N/K250Q double mutant (C) Camuiα in cell lysate after CFP specific excitation before and after addition of Ca^{2+}/CaM was detected, followed by 4 μg/mL of nano-C60 treatment or not, and then 10 mM EGTA. (D). The FRET level of wild type and D246N/K250Q double mutant Camuiα in dendrites of cultured neurons by application of nano-C60 or nanodiamond. The upper panel showed the high-magnification FRET images of the dendrites before and after nano-C60 or nanodiamond stimulation. Scale bar indicates 1 μm. Images are shown in intensity-modulated display mode, in which a warmer hue indicates a higher CFP/YFP ratio or lower FRET. The lower panel showed the ensemble change in FRET level, which is the average of three images taken in every 5 min and was normalized to unstimulated level. The arrows indicate the addition of 0.2 μg/mL of nano-C60 or nandiamond.

Combined with the binding and dissociation data (Figure 2, C and D) showing the higher affinity of nano-C60 toward the activated CaMKII than the basal-state CaMKII, these results also strongly suggested that nano-C60-bound CaMKIIα, once activated, would remain in the active conformation as the binding prevents the reassociation of the autoinhibitory sequence with the catalytic domain regardless whether Ca^{2+}/CaM is present, thus offering a likely explanation for the observed CaMKII locking effect.

DISCUSSION

On the basis of our results, we propose a working model to account for nano-C60s action on CaMKII (Scheme 1). CaMKII holoenzyme, normally present in an autoinhibited basal state, binds to distinct sites on the surface of internalized nano-C60 through exposed epitopes defined by specific amino acid residues including aspartic acid 246 (D246) and lysine 250 (K250) in the catalytic domain of the CaMKIIα subunit. Once a Ca^{2+} stimulus activates the nano-C60-bound CaMKII through the well-known mechanism of releasing the autoinhibitory domain, nano-C60 locks the kinase in an active conformation by preventing the reassociation of the autoinhibitory domain with the catalytic domain, analogous to the locking effect elicited by Threonine 286 (T286) autophosphorylation or NR2B binding. The highly stable and persistent binding of activated CaMKIIα to nano-C60 ensures that all of the CaMKII subunits within a nano-C60-bound CaMKII holoenzyme would be activated, through intersubunit T286 (T287 for CaMKIIβ) autophosphorylation, and remain in the activated state even after the Ca^{2+} stimulus is withdrawn, for as long as the nano-C60 is in place.

The results from this work revealed several important insights regarding protein−nanoparticle interactions in a cellular environment. We showed that the surface of nano-C60 is heterogeneous, possessing distinct binding sites for CaMKII. The presence of such distinct binding sites for a particular protein, or a set of proteins, may be a common feature for many inorganic nanoparticles and provides a distinctive biological

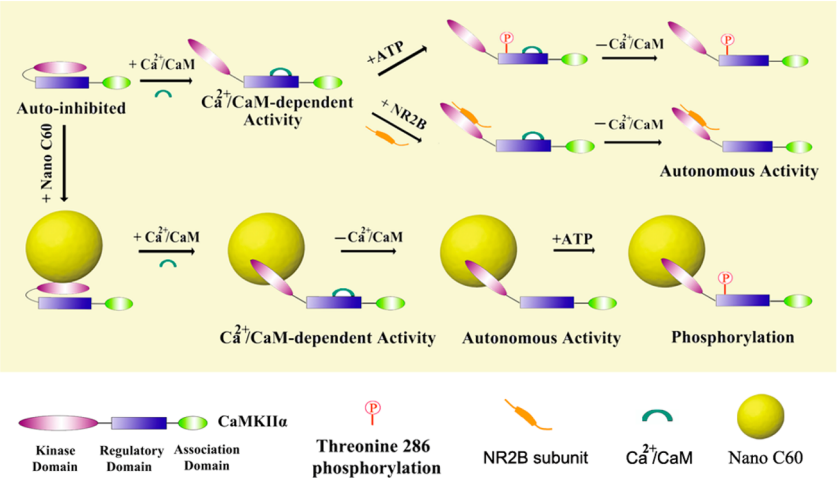

Scheme 1. Schematic diagram illustrating the currently known mechanisms for generating Ca^{2+}/CaM-autonomous activity of CaMKII in the brain, achieved by T286 autophosphorylation, binding to NR2B, and binding to nano-C60, respectively. Only one CaMKIIα subunit for the CaMKII holoenzyme is shown.

identity for the nanoparticle. Furthermore, the interaction of proteins with these distinct sites is likely to be highly specific and dictated by particular epitopes or conformations displayed by the protein. In this study, a change of two amino acid residues was sufficient to confer the complete loss-of-binding for CaMKII, demonstrating the stringent specificity for CaMKII−nano-C60 interaction. Finally, the interaction of a nanoparticle with a cellular protein may provide robust modulation on the protein, both structurally and functionally. As there are thousands of cellular signaling proteins and millions of protein−protein interactions, the potential capacity for nanoparticles to modulate these signaling processes is enormous.

Our results also demonstrated the surprising capability of an inorganic nanoparticle to act like a signaling protein in transmitting signals through interacting with another signaling protein. The ability of nano-C60 to sustain Ca^{2+}/CaM-independent activity of CaMKII is reminiscent of NR2B protein, which binds to specific residues in the catalytic domain of Ca^{2+}/CaM-activated CaMKII and prevents the reassociation of the unphosphorylated T286, located in the autoinhibitory domain, with a noncatalytic site (T site) within the catalytic domain, thus keeping CaMKII constitutively active even after the withdrawal of Ca^{2+}/CaM.[32,43] And analogous to nano-C60−CaMKII interaction, NR2B−CaMKII interaction also leads to CaM trapping and CaMKII postsynaptic translocation.[32] While interaction of CaMKII with either nano-C60 or NR2B has the same consequence of locking the kinase in an active conformation, there are several remarkable differences between these two types of interactions. NR2B binds to CaMKII only after Ca^{2+}/CaM activation, while both basal and activated CaMKII can bind to nano-C60, although activated CaMKII binds more strongly. In neurons, binding of NR2B to CaMKII is reversible and transient, lasting from seconds to minutes,[43] but the binding of CaMKII to nano-C60 lasts for hours, as dissociation of CaMKII from nano-C60 is very slow and nano-C60 inside the cell may not be easily eliminated. Moreover, interaction of NR2B with CaMKII occurs in a one-to-one fashion, while multiple (up to thousands) of CaMKII molecules bind to one nano-C60 nanoparticle. Thus, binding of CaMKII to nano-C60 may lead to high concentration of activated CaMKII in localized regions within a cell.

As CaMKII is a multifunctional kinase involved in many cellular processes, the generation of Ca^{2+}/CaM-autonomous CaMKII activity for an extended period of time by nano-C60 may have a plethora of physiological effects in different tissues and organs and represents a double-edged sword for *in vivo* applications of fullerene C60. On the one hand, the prolonged activation of CaMKII raises safety concerns, as abnormally activated CaMKII has been associated with heart disease,[44] asthma[45] and other toxicity issues such as cell death.[46] On the other hand, ability of nano-C60 to sustain the Ca^{2+}/CaM-autonomous CaMKII activity might, in theory, provide a beneficial effect in certain situations. Notably, dysfunction of CaMKII has been shown in many studies to concur with memory loss in neurodegenerative diseases such as Alzheimer's disease and Parkinson's disease, thus it would be interesting to see if the sustained autonomous CaMKII activity elicited by nano-C60 in hippocampal neurons might have any effect on learning and memory in general and on neurodegenerative diseases in particular. Further studies are needed to address these possibilities.

CONCLUSION

In this work we revealed a hitherto unrecognized ability of C60 nanocrystals, in a fashion highly analogous to the neuronal signaling protein NR2B, to

specifically interact with a set of amino acid residues within the catalytic domain of CaMKIIα, thus locking the protein in an active conformation upon activation and leading to robust functional modulations including sustained autonomous kinase activity, CaM trapping and postsynaptic translocation.

MATERIALS AND METHODS

Materials. Ultrapure water (pH 6.7; Milli-Q, Bedford, MA) was used in all situations throughout the experiments. pcDNA3.1-CaMKIIα, GFP-CaMKIIα and GFP-CaMKIIβ, were kind gifts from Tatsuo Suzuki (Shinshu University, Japan) and Howard Schulman (Stanford University, USA). Camuiα was kind gift from Yasunori Hayashi (Massachusetts Institute of Technology, USA). Fullerene C60 (99.9% pure), Fullerenol (Polyhydroxy-C60) was purchased from Bucky USA (Houston, USA). Single-walled carbon nanotube (SWCNT) (Cat. No. 519308), nanodiamond (Cat. No. 636428), Genistein (Cat. No. 446−72−0), dimethyl amiloride (DMA) (Cat. No. 1214−79−5) and Hoechst 33342 (B2261) were form Sigma-Aldrich. Syntide-2 (Cat. No. 05−23−4910), Bovine Calmodulin (Cat. No. 208690), Porcine Calmodulin (Cat. No. 208783), Porcine Rhodamine-Calmodulin (Cat. No. 208781) were purchased from Calbiochem. Antibodies against total CaMKII (Cat. No. sc-9035), CaMKIIα (Cat. No. sc-1314) and C60 (sc69901) were purchased from Santa Cruz Biotechnology. CaMKIIβ antibody (Cat. No. 13−9800) was from Invitrogen. His-tag antibody (2A8; Cat. No. 214574) was purchased from Abmart (Shanghai, China, http://www.ab-mart.com). Antiphospho CaMKII antibody (Cat. No. V1111) and Halotag protein purification system (Cat. No. G6270) were purchased from Promega. Alexa Fluor 594 AffiniPure Goat antimouse IgG was purchased from Jackson ImmunoResearch Laboratories (USA). GAPDH antibody (Cat. No. MAB374) and P81 phosphocellulose paper were purchased from Millipore. Calmodulin Sepharose 4B (Cat. No. 17−0529−01) was from GE Healthcare Life Sciences. QuikChange Lightning Site-Directed Mutagenesis Kit (Cat. No. 210518) was purchased from Stratagene. γ-^{32}P-ATP was purchased from Beijing Furui Biological Engineering Company (Beijing, China; http://www.bjfrsw.com/). CaMKII assay kit (CY-1173) was purchased from CycLex (Nagano, Japan).

Nanoparticles Preparation. Nano-C60 in water suspension was prepared as described previously.[27] The obtained nano-C60 suspension was analyzed by HPLC and the accurate concentration was found to be about 40 μg/mL. Aqueous suspension of nanodiamond and single-walled carbon nanotube with the concentration of 1 mg/mL were prepared by dissovling in double distilled water followed by ultrasonic treatment for 30 min. These nanoparticles were characterized by transmission electron microscopy (TEM) (JEOL-2010).

Nanoparticle Number Determination. Nano-C60 suspension was injected into the analyzer of Nanoparticle Tracking Analysis (NanoSight LM10, NanoSight Ltd., England). The nano-C60 suspension was found to contain about $6.255 \times 10^{10} \pm 0.64374$ nanoparticles/mL, which translated to about 1.56×10^9 nanoparticles per μg of nano-C60.

Protein Expression in Cells. pcDNA3.1-CaMKIIβ for expressing the full length rat CaMKIIβ protein in mammalian cells was constructed by PCR amplification with primers P1 (CGCGGATCCATGGCCACCACGGTGACCTG) and P2 (CTAGTCTAGAACTGCAGTGGGGCCACTGGA) using GFP-CaMKIIβ as the template, followed by subcloning into pcDNA3.1. pcDNA3.1-CaMKIIα was kindly provided by Tatsuo Suzuki. The mutations of H84F, P189A, D246N, K250Q and D246N/K250Q in CaMKIIα were generated by the site-directed mutagenesis kit (Stratagene) according to the manufacturer's protocol using the pcDNA3.1-CaMKIIα plasmid as a template. The D246N/K250Q mutant was also generated using template of Camuiα plasmids. Camuiα with cyan fluorescent protein (CFP) and yellow fluorescent protein (YFP) at each end has been described previously[42] and was kindly provided by Yasunori Hayashi. All plasmids were verified by sequencing. COS-7 and human embryonic kidney 293T (HEK293T) cells, maintained continuously as a monolayer at 37 °C and 5% CO_2 in Dulbecoo's Modified Eagle's Medium (DMEM) supplemented with 10% FBS, were grown to about 80% confluency. COS-7 cells were transiently transfected with pcDNA3.1-CaMKIIα, pcDNA3.1-CaMKIIβ and pcDNA3.1-CaMKIIα mutants (H84F, P189A, D246N, K250Q and D246N/K250Q) respectively, using Lipofectamine 2000 (Invitrogen). HEK293T cells were transiently transfected with Camuiα. After transfection, cells were collected and disrupted by Cell Lysis Buffer (P0013, Beyotime, China). Cell extracts were centrifuged at 12000*g* for 30 min at 4 °C and the supernatant was frozen at −80 °C until just prior to use. Protein concentrations were determined by the BCA protein assay.

Protein Expression and Purification in *E. coli*. The plasmids for expressing the full length rat CaMKIIα and CaMKIIβ proteins were constructed with pFN18A Halotag T7 Flexi Vector (Promega) using GFP-CaMKIIα and GFP-CaMKIIβ as PCR templates, respectively. The primers used were P3 and P4 for CaMKIIα, and P5 and P6 for CaMKIIβ. His-tagged full length CaMKIIα, α1 (1−273), α2 (274−478) and α3 (313−478) proteins were expressed in *E. coli* in the pET22b(+) vector (Novagen) system, using GFP-CaMKIIα as the template. The respective PCR primers were as follows: P7 and P10 for full length CaMKIIα, P7 and P8 for α1, P9 and P10 for α2, and P11 and P10 for α3. All plasmids were verified by sequencing. The primer sequences were as follows:

P3 CATGGCGATCGCCATGGCTACCATCACCTGCACC

P4 CGCGTTTAAACTCAATGGGGCAGGACGGAG

P5 CATGGCGATCGCCATGGCCACCACGGTGACCTG

P6 CGCGTTTAAACTTACTGCAGTGGGGCCACTGG

P7 GGAATTCCATATGGCTACCATCACCTGCACC

P8 CCGCTCGAGGTGCGAGATCCAGGGGTGC

P9 GGAATTCCATATGCGCTCCACTGTGGCCTCCT

P10 CCGCTCGAGATGGGGCAGGACGGAG

P11 GGAATTCCATATGTTCTCCGGAGGGAAGAGTGGA

E. coli harboring the Halotag expression plasmids were grown to early log phase, induced with 0.05% rhamnose for 20 h. Soluble proteins were prepared and loaded on HaloLink resin, and the target proteins were released by cleaving with Tobacco Etch Virus Protease (TEV), following manufacturer's instructions. His-tagged proteins were overproduced in *E. coli* BL21 (DE3) with 1 mM IPTG induction for 3 h at an optical density of 0.7 (wavelength 600 nm) and purified by Ni^{2+} affinity chromatography according to the Novagen technical manual.

Preparation of Partially Purified CaMKII from Rat Hippocampus. Rat brain kinase was partially purified as described by Bennett *et al.*[47] Fresh forebrains were removed from SD rats and homogenized immediately with Teflon glass homogenizer in 10 volumes of buffer A (20 mM Tris (pH 7.5), 1 mM DTT, 1 mM EDTA, 1 mM EGTA, 0.1 mM PMSF, 5 μg/mL soybean trypsin inhibitor, 20 μg/mL leupeptin), The homogenate was centrifuged at 17000*g* at 4 °C for 30 min, and the resulting supernatant was centrifuged at 17000*g* for 1h. The supernatant fraction was loaded onto a DEAE−cellulose column (DE-52) pre-equilibrated with buffer A at 4 °C. The column was washed with five column volume of buffer A containing 50 mM NaCl. The protein was eluted with a linear gradient of 50 to 200 mM NaCl in buffer A. Peak fractions were pooled and brought to 50% saturation by the slow addition of solid ammonium sulfate over 1 h on ice. After 3 h, precipitated protein was collected by centrifugation, resuspended in 5 mL of Buffer B (20 mM Tris (pH 7.5), 1.5 mM $CaCl_2$, 1 mM DTT, 200 mM NaCl, 0.1 mM PMSF) and loaded on a calmodulin−agarose affinity column pre-equilibrated with buffer B at 4 °C. The column was washed with five column volumes of buffer B containing 1 M NaCl and then the enzyme was eluted with Buffer C (20 mM Tris (pH 7.5), 2 mM EGTA, 200 mM NaCl, 1 mM DTT, 0.1 mM PMSF).

The thus-obtained CaMKII was dialyzed into 20 mM Tris (pH 7.5) and then frozen in aliquots at −80 °C. Protein concentrations were measured by BCA Protein Assay Kit.

Nano-C60 Binding Assays. In a typical assay, nano-C60 was added to a protein sample, incubated at 4 °C for 2 h or the indicated times for the time course studies, and then centrifuged at 12000*g* for 30 min. The supernatant was saved while the pellet was washed 3 times with PBS containing 3% tween 20. The starting protein sample, the supernatant and the pellet, respectively, were boiled for 10 min in the SDS loading buffer, followed by SDS-PAGE and Western blotting with appropriate antibodies. For assessing the effect of Ca^{2+}/CaM activation and phosphorylation on nano-C60 binding, forebrain lysate was treated with 500 μM $CaCl_2$ and 1 μM CaM, with or without 1 mM ATP, for 30 min on ice before the addition of nano-C60.

Dissociation Assays. A CaMKII-bound nano-C60 pellet was prepared following the binding procedure described above, using 6 μg of nano-C60 and 1 mL of forebrain lysate (6 mg/mL in protein concentration). The pellet was washed for 3 times with 20 mM Tris (pH 7.5), resuspened in 150 μL of 20 mM Tris, and then divided into three equal portions. These portions were untreated, treated with Ca^{2+}/CaM (500 μM $CaCl_2$ and 1 μM CaM), or with Ca^{2+}/CaM, 10 mM $MgCl_2$ and 1 mM ATP for 30 min. At the various times after treatment, an aliquot was withdrawn and centrifuged, with the supernatant and pellet collected for subsequent Western blotting.

CaMKII Kinase Assays. For detecting CaMKII activity *in vitro*, assays were performed in a final volume of 50 μL. Partially purified rat forebrain CaMKII with a protein concentration of 0.1 mg/mL (final concentration) was pretreated with a buffer containing 50 mM Hepes (pH 7.5), 10 mM $MgCl_2$ and 30 μM synthetic substrate syntide-2 (for activating kinase, this buffer also contains 500 μM $CaCl_2$ and 1 μM CaM) on ice for 1 min. 4 μg/mL nano-C60 was added and incubated for 20 min followed by treatment with 10 mM EGTA for 10 min on ice. The kinase reactions were initiated by the addition of 10 μM ATP containing 5 μCi γ-^{32}P-ATP and run for 2 min at 30 °C. 15 μL of the reaction was spotted on Whatman P81 phosphocellulose paper. The paper was washed with water for 5 times, dried and then quantified for radioactivity with a liquid scintillation counter (Beckman LS1701 analyzer). The amount of radioactivity produced by the basal-state CaMKII (without Ca^{2+}/CaM and without nano-C60) was set at 1 and used to normalize the relative activity for other treatments. For detecting the activity of wild type, D246N/K250Q or T286A mutant CaMKIIα in COS-7 cell lysate, assays were performed using the CycLex CaMKII assay kit. Cell extracts were treated with 1.5 mM $CaCl_2$ and 3 μM CaM on ice for 1 min, followed by the treatment with or without 4 μg/mL nano-C60 on ice for 20 min. The mixture was then diluted 1:10 in the kinase buffer in the kit with 1 mM EGTA and loaded onto wells coated with Syntide-2. The absorbance at 450 nm was measured with a spectrophotometer (Elx800, BioTek, USA).

CaMKII Autophosphorylation. CaMKII autophosphorylation at T286 was analyzed by immunoblotting using antiphospho CaMKII antibody. Lysates from COS-7 cells transfected with wild type or D246N/K250Q double mutant CaMKIIα were pretreated with 500 μM $CaCl_2$, 1 μM CaM and 10 mM $MgCl_2$ on ice for 1 min. 4 μg/mL nano-C60, nanodiamond was respectively added and incubated for 20 min followed by treatment with 1 mM EGTA for 10 min on ice. The CaMKII phosphorylation was initiated by the addition of 1 mM ATP, and stopped after 30 min with SDS loading buffer. For detecting CaMKII activity *in vivo*, 0.2 μg/mL nanoparticles were incubated with COS-7 cells transfected with wild type or D246N/K250Q double mutant CaMKIIα or HT22 hippocampal neuronal cells (HT22) for 1 h. The phosphorylated CaMKII was detected by SDS-PAGE followed by Western blotting with antibodies against CaMKII and phospho-CaMKII.

CaMKII-CaM Affinity Detection. Lysate from COS-7 cells transfected with CaMKIIα was loaded on Calmodulin Sepharose pre-equilibrated with buffer A (20 mM Tris (pH 7.5), 200 mM NaCl, 2 mM $CaCl_2$) at 4 °C for 2 h. Then the Calmodulin Sepharose was washed with buffer A for three times, and then buffer B (20 mM Tris (pH 7.5), 2 mM $CaCl_2$) for two times, followed by incubation with or without 8 μg/mL nano-C60 at 4 °C for 30 min. After centrifugation, the Calmodulin Sepharose was incubated with buffer C (20 mM Tris (pH 7.5), 2 mM $CaCl_2$, 20 μM CaM), in which excessive amount of CaM initiated the dissociation of CaMKIIα from Calmodulin Sepharose. Then the Calmodulin Sepharose was washed with 20 mM Tris (pH 7.5) for once after 15 min, followed by adding SDS-loading buffer for subsequent Western blotting.

Rhodamine-Calmodulin Dissociation Assay. The dissociation of porcine Rhodamine-Calmodulin (R-CaM) from partially purified rat forebrain CaMKII was measured in SpectraMax M5 (Molecular Devices Corporation, California). The measurement was performed at 25 °C. Excitation was at 552 nm, and the emission maximum was at 575 nm. The assays contained 10 mM Tris (pH 7.4), 650 nM CaMKIIα, 500 μM $CaCl_2$, 5 mM $MgCl_2$, 25 nM R-CaM, 100 μM EGTA, 7.5 μM unlabeled porcine CaM and 4 mM ATP or 4 μg/mL nano-C60. To measure the dissociation of R-CaM from autophosphorylated or nano-C60-bound CaMKII, ATP or nano-C60 was added to the well already containing Ca^{2+}, R-CaM and CaMKII. After the fluorescence intensity reaching a steady state, 300-fold excess unlabeled CaM (7.5 μM) was added to initiate dissociation of R-CaM and the changes in fluorescence were monitored.

Fluorescence Resonance Energy Transfer (FRET). Lysate from HEK293T cells transfected with wild type or D246N/K250Q double mutant Camuiα (3 mg/mL in protein concentration) was used as the source of the enzyme for the subsequent FRET detecting. 4 μg/mL (final concentration) nano-C60 or nanodiamond was incubated with HEK293T cell lysate containing wile type Camuiα at 4 °C for 30 min and then centrifuged at 12000*g* for 30 min. The pellets were resuspended in the same volume of supernatant by Cell Lysis Buffer. To stimulate the wild type Camuiα, 2 mM $CaCl_2$ and 3 μM CaM were added in the cell lysate, resuspended nano-C60 or nanodiamond pellet at room temperature. The reaction was stopped by 10 mM EGTA. The effect of nano-C60 on D246N/K250Q double mutant Camuiα was also been detected. Wild type or D246N/K250Q double mutant Camuiα in cell lysate was incubated with 2 mM $CaCl_2$ and 3 μM CaM, followed by the addition of 4 μg/mL nano-C60, and then 10 mM EGTA. FRET was measured using an excitation wavelength at 433 nm for CFP under Spectrofluorophotometer (RF-5301, Shimadzu corporation, Japan). FRET level is expressed throughout as a ratio of emissions at 486 nm (CFP) to 535 nm (YFP), in which a higher value indicates less FRET.

Immunofluorescence. HT22 cells were seeded on coverslips in 24-well plates. To determine the uptake mechanism of nano-C60 into neurons, HT22 cells were pretreated with or without genistein (200 μM) or dimethyl amiloride (DMA,100 μM) for 1 h at 37 °C. After removing the inhibitors through changing the DMEM, nano-C60 was added and incubated with the cells for another 1 h. The cells were then fixed by 4% paraformaldehyde for 10 min at room temperature. After permeabilization in 0.1% Triton X-100 for 10 min and preblocking in PBS with 2% fetal bovine serum (v/v) and 3% BSA (w/v) for 1 h, cells were incubated with C60 antibodies overnight at 4 °C and then with Alexa Fluor 594 AffiniPure Goat antimouse IgG for 1 h at room temperature. After staining with Hoechst 33342 for nuclei, the coverslips were placed on microscopy slides with a drop of Gold antifade reagent (Invitrogen) and then sealed. Cells were observed under fluorescent microscopy (Olympus IX71, Olympus, Japan).

Neuron Imaging. Primary cultures of hippocampal neurons were prepared as described previously.[48] FRET imaging and CaMKII translocation in neurons were observed by using a Zeiss LSM710 (Carl Zeiss Inc., Thornwood, NY) equipped with 63× oil-immersion objectives.[42,49] Argon laser excitation wavelengths were 458 nm for CFP, 535 nm for YFP and 488 nm for GFP. Hippocampal neurons were transfected by the Ca^{2+}-phosphate method (at 7−11 d *in vitro*) and imaged at 12−14 d *in vitro* in solution containing the following (in mM): 145 NaCl, 3 KCl, 1.2 $CaCl_2$, 1.2 $MgCl_2$, 10 glucose, and 10 HEPES-Na, pH 7.4. Image-J software was used for image analysis. After stimulation with 50 μM glutamate, 0.2 μg/mL nano-C60 or 0.2 μg/mL nanodiamond, the FRET images were observed and the FRET level was displayed in intensity-modulated display mode, where warmer hue indicates a higher CFP/YFP ratio or less FRET.

For detecting CaMKIIα translocation in hippocampal neurons, the neurons were transfected with GFP-CaMKIIα and the distribution of GFP-CaMKIIα was analyzed by the fluorescence intensity of GFP.

Statistical Analysis. All data were represented as mean ± SEM. Statistical analysis method used was two-tailed student's *t* tests for all other data. Probabilities of less than 0.05 were considered significant.

Conflict of Interest: The authors declare no competing financial interest.

Acknowledgment. This work was supported by grants from the National Basic Research Program of China (2013CB933902), the National Natural Science Foundation of China (31071211, 31170966, 51201034), and the Young Scientist Innovation Fund of USTC (WK2340000045, WK2070000031). We thank Howard Schulman for providing GFP-CaMKIIα and GFP-CaMKIIβ, Tatsuo Suzuki for pcDNA3.1-CaMKIIα, and Yasunori Hayashi for Camuiα plasmids. We also thank H. Liu (University of Science and Technology of China) for assisting with drawing the CaMKII structure, X. Wan, C. Wang and P. Jin (University of Science and Technology of China) for their useful discussions.

Supporting Information Available: Characterization of nanoparticles with TEM, LC−MS/MS results, nano-C60-binding proteins identification, effect of protein corona around nano-C60 on nano-C60−CaMKIIα interaction, effect of photoirradiation on nano-C60−CaMKIIα interaction, competitive binding experiment, sequence alignment among catalytic domain of rat CaMKII, structure of CaMKII, effect of nanoparticles on the CaMKIIα activity, as well as effects of glutamate on the FRET of Camuiα in the neurons. This material is available free of charge *via* the Internet at http://pubs.acs.org.

REFERENCES AND NOTES

1. Lynch, I.; Dawson, K. A. Protein-Nanoparticle Interactions. *Nano Today* **2008**, *3*, 40–47.
2. Mahmoudi, M.; Lynch, I.; Ejtehadi, M. R.; Monopoli, M. P.; Bombelli, F. B.; Laurent, S. Protein-Nanoparticle Interactions: Opportunities and Challenges. *Chem. Rev.* **2011**, *111*, 5610–5637.
3. Nel, A. E.; Madler, L.; Velegol, D.; Xia, T.; Hoek, E. M. V.; Somasundaran, P.; Klaessig, F.; Castranova, V.; Thompson, M. Understanding Biophysicochemical Interactions at the Nano-Bio Interface. *Nat. Mater.* **2009**, *8*, 543–557.
4. Shemetov, A. A.; Nabiev, I.; Sukhanova, A. Molecular Interaction of Proteins and Peptides with Nanoparticles. *ACS Nano* **2012**, *6*, 4585–4602.
5. Cedervall, T.; Lynch, I.; Lindman, S.; Berggard, T.; Thulin, E.; Nilsson, H.; Dawson, K. A.; Linse, S. Understanding the Nanoparticle-Protein Corona Using Methods to Quantify Exchange Rates and Affinities of Proteins for Nanoparticles. *Proc. Natl. Acad. Sci. U. S. A.* **2007**, *104*, 2050–2055.
6. Monopoli, M. P.; Aberg, C.; Salvati, A.; Dawson, K. A. Biomolecular Coronas Provide the Biological Identity of Nanosized Materials. *Nat. Nanotechnol.* **2012**, *7*, 779–786.
7. Asuri, P.; Bale, S. S.; Karajanagi, S. S.; Kane, R. S. The Protein-Nanomaterial Interface. *Curr. Opin. Biotechnol.* **2006**, *17*, 562–568.
8. Zuo, G. H.; Huang, Q.; Wei, G. H.; Zhou, R. H.; Fang, H. P. Plugging into Proteins: Poisoning Protein Function by a Hydrophobic Nanoparticle. *ACS Nano* **2010**, *4*, 7508–7514.
9. Shen, J. W.; Wu, T.; Wang, Q.; Kang, Y. Induced Stepwise Conformational Change of Human Serum Albumin on Carbon Nanotube Surfaces. *Biomaterials* **2008**, *29*, 3847–3855.
10. Shang, W.; Nuffer, J. H.; Dordick, J. S.; Siegel, R. W. Unfolding of Ribonuclease A on Silica Nanoparticle Surfaces. *Nano Lett.* **2007**, *7*, 1991–1995.
11. Song, M. Y.; Jiang, G. B.; Yin, J. F.; Wang, H. L. Inhibition of Polymerase Activity by Pristine Fullerene Nanoparticles Can Be Mitigated by Abundant Proteins. *Chem. Commun.* **2010**, *46*, 1404–1406.
12. Vertegel, A. A.; Siegel, R. W.; Dordick, J. S. Silica Nanoparticle Size Influences the Structure and Enzymatic Activity of Adsorbed Lysozyme. *Langmuir* **2004**, *20*, 6800–6807.
13. Deng, Z. J.; Liang, M. T.; Monteiro, M.; Toth, I.; Minchin, R. F. Nanoparticle-Induced Unfolding of Fibrinogen Promotes Mac-1 Receptor Activation and Inflammation. *Nat. Nanotechnol.* **2011**, *6*, 39–44.
14. Lynch, I.; Dawson, K. A.; Linse, S. Detecting Cryptic Epitopes Created by Nanoparticles. *Sci. STKE* **2006**, *2006*, 14.
15. Linse, S.; Cabaleiro-Lago, C.; Xue, W. F.; Lynch, I.; Lindman, S.; Thulin, E.; Radford, S. E.; Dawson, K. A. Nucleation of Protein Fibrillation by Nanoparticles. *Proc. Natl. Acad. Sci. U. S. A.* **2007**, *104*, 8691–8696.
16. Shang, W.; Nuffer, J. H.; Muniz-Papandrea, V. A.; Colon, W.; Siegel, R. W.; Dordick, J. S. Cytochrome c on Silica Nanoparticles: Influence of Nanoparticle Size on Protein Structure, Stability, and Activity. *Small* **2009**, *5*, 470–476.
17. Prigodich, A. E.; Alhasan, A. H.; Mirkin, C. A. Selective Enhancement of Nucleases by Polyvalent DNA-Functionalized Gold Nanoparticles. *J. Am. Chem. Soc.* **2011**, *133*, 2120–2123.
18. Corgie, S. C.; Kahawong, P.; Duan, X. N.; Bowser, D.; Edward, J. B.; Walker, L. P.; Giannelis, E. P. Self-Assembled Complexes of Horseradish Peroxidase with Magnetic Nanoparticles Showing Enhanced Peroxidase Activity. *Adv. Funct. Mater.* **2012**, *22*, 1940–1951.
19. Calzolai, L.; Franchini, F.; Gilliland, D.; Rossi, F. Protein-Nanoparticle Interaction: Identification of the Ubiquitin-Gold Nanoparticle Interaction Site. *Nano Lett.* **2010**, *10*, 3101–3105.
20. Kotov, N. A. Inorganic Nanoparticles as Protein Mimics. *Science* **2010**, *330*, 188–189.
21. Hayder, M.; Poupot, M.; Baron, M.; Nigon, D.; Turrin, C. O.; Caminade, A. M.; Majoral, J. P.; Eisenberg, R. A.; Fournie, J. J.; Cantagrel, A.; *et al.* A Phosphorus-Based Dendrimer Targets Inflammation and Osteoclastogenesis in Experimental Arthritis. *Sci. Transl. Med.* **2011**, *3*, 81ra35.
22. Teo, I.; Toms, S. M.; Marteyn, B.; Barata, T. S.; Simpson, P.; Johnston, K. A.; Schnupf, P.; Puhar, A.; Bell, T.; Tang, C.; *et al.* Preventing Acute Gut Wall Damage in Infectious Diarrhoeas with Glycosylated Dendrimers. *EMBO Mol. Med.* **2012**, *4*, 866–881.
23. De, M.; Chou, S. S.; Dravid, V. P. Graphene Oxide as an Enzyme Inhibitor: Modulation of Activity of Alpha-Chymotrypsin. *J. Am. Chem. Soc.* **2011**, *133*, 17524–17527.
24. Kroto, H. W.; Heath, J. R.; Obrien, S. C.; Curl, R. F.; Smalley, R. E. C-60—Buckminsterfullerene. *Nature* **1985**, *318*, 162–163.
25. Zhang, Q. M.; Yi, J. Y.; Bernholc, J. Structure and Dynamics of Solid C60. *Phys. Rev. Lett.* **1991**, *66*, 2633–2636.
26. Bosi, S.; Da Ros, T.; Spalluto, G.; Prato, M. Fullerene Derivatives: an Attractive Tool for Biological Applications. *Eur. J. Med. Chem.* **2003**, *38*, 913–923.
27. Zhang, Q.; Yang, W. J.; Man, N.; Zheng, F.; Shen, Y. Y.; Sun, K. J.; Li, Y.; Wen, L. P. Autophagy-Mediated Chemosensitization in Cancer Cells by Fullerene C60 Nanocrystal. *Autophagy* **2009**, *5*, 1107–1117.
28. Park, K. H.; Chhowalla, M.; Iqbal, Z.; Sesti, F. Single-Walled Carbon Nanotubes Are a New Class of Ion Channel Blockers. *J. Biol. Chem.* **2003**, *278*, 50212–50216.
29. Jin, H.; Chen, W. Q.; Tang, X. W.; Chiang, L. Y.; Yang, C. Y.; Schloss, J. V.; Wu, J. Y. Polyhydroxylated C(60), Fullerenols, as Glutamate Receptor Antagonists and Neuroprotective Agents. *J. Neurosci. Res.* **2000**, *62*, 600–607.
30. Dugan, L. L.; Turetsky, D. M.; Du, C.; Lobner, D.; Wheeler, M.; Almli, C. R.; Shen, C. K. F.; Luh, T. Y.; Choi, D. W.; Lin, T. S. Carboxyfullerenes as Neuroprotective Agents. *Proc. Natl. Acad. Sci. U. S. A.* **1997**, *94*, 12241–12241.
31. Calvaresi, M.; Zerbetto, F. Baiting Proteins with C-60. *ACS Nano* **2010**, *4*, 2283–2299.
32. Bayer, K. U.; De Koninck, P.; Leonard, A. S.; Hell, J. W.; Schulman, H. Interaction with the NMDA Receptor Locks CaMKII in an Active Conformation. *Nature* **2001**, *411*, 801–805.
33. Hudmon, A.; Schulman, H. Neuronal Ca^{2+}/Calmodulin-Dependent Protein Kinase II: The Role of Structure and Autoregulation in Cellular Function. *Annu. Rev. Biochem.* **2002**, *71*, 473–510.
34. Chao, L. H.; Stratton, M. M.; Lee, I. H.; Rosenberg, O. S.; Levitz, J.; Mandell, D. J.; Kortemme, T.; Groves, J. T.; Schulman, H.; Kuriyan, J. A Mechanism for Tunable Autoinhibition in the

Structure of a Human Ca^{2+}/Calmodulin-Dependent Kinase II Holoenzyme. *Cell* **2011**, *147*, 704–704.
35. Bayer, K. U.; LeBel, E.; McDonald, G. L.; O'Leary, H.; Schulman, H.; De Koninck, P. Transition from Reversible to Persistent Binding of CaMKII to Postsynaptic Sites and NR2B. *J. Neurosci.* **2006**, *26*, 1164–1174.
36. Meyer, T.; Hanson, P. I.; Stryer, L.; Schulman, H. Calmodulin Trapping by Calcium-Calmodulin Dependent Protein-Kinase. *Science* **1992**, *256*, 1199–1202.
37. Putkey, J. A.; Waxham, M. N. A Peptide Model for Calmodulin Trapping by Calcium/Calmodulin-Dependent Protein Kinase II. *J. Biol. Chem.* **1996**, *271*, 29619–29623.
38. Waxham, M. N.; Tsai, A. L.; Putkey, J. A. A Mechanism for Calmodulin (CaM) Trapping by CaM-Kinase II Defined by a Family of CaM-Binding Peptides. *J. Biol. Chem.* **1998**, *273*, 17579–17584.
39. Parton, R. G.; Joggerst, B.; Simons, K. Regulated Internalization of Caveolae. *J. Cell. Biol.* **1994**, *127*, 1199–1215.
40. Raoof, M.; Mackeyev, Y.; Cheney, M. A.; Wilson, L. J.; Curley, S. A. Internalization of C60 Fullerenes into Cancer Cells with Accumulation in the Nucleus *via* the Nuclear Pore Complex. *Biomaterials* **2012**, *33*, 2952–2960.
41. Strack, S.; Choi, S.; Lovinger, D. M.; Colbran, R. J. Translocation of Autophosphorylated Calcium/Calmodulin-Dependent Protein Kinase II to the Postsynaptic Density. *J. Biol. Chem.* **1997**, *272*, 13467–13470.
42. Takao, K.; Okamoto, K. I.; Nakagawa, T.; Neve, R. L.; Nagai, T.; Miyawaki, A.; Hashikawa, T.; Kobayashi, S.; Hayashi, Y. Visualization of Synaptic Ca^{2+}/Calmodulin-Dependent Protein Kinase II Activity in Living Neurons. *J. Neurosci.* **2005**, *25*, 3107–3112.
43. Lisman, J.; Schulman, H.; Cline, H. The Molecular Basis of CaMKII Function in Synaptic and Behavioural Memory. *Nat. Rev. Neurosci.* **2002**, *3*, 175–190.
44. Anderson, M. E.; Brown, J. H.; Bers, D. M. CaMKII in Myocardial Hypertrophy and Heart Failure. *J. Mol. Cell. Cardiol.* **2011**, *51*, 468–473.
45. Sanders, P. N.; Koval, O. M.; Jaffer, O. A.; Prasad, A. M.; Businga, T. R.; Scott, J. A.; Hayden, P. J.; Luczak, E. D.; Dickey, D. D.; Allamargot, C.; *et al.* CaMKII Is Essential for the Proasthmatic Effects of Oxidation. *Sci. Transl. Med.* **2013**, *5*, 195ra97.
46. Bissonnette, S. L.; Haas, A.; Mann, K. K.; Schlezinger, J. J. The Role of CaMKII in Calcium-Activated Death Pathway in Bone Marrow B Cells. *Toxicol. Sci.* **2010**, *118*, 108–118.
47. Bennett, M. K.; Erondu, N. E.; Kennedy, M. B. Purification and Characterization of a Calmodulin-Dependent Protein-Kinase That Is Highly Concentrated in Brain. *J. Biol. Chem.* **1983**, *258*, 2735–2744.
48. Bi, G. Q.; Poo, M. M. Synaptic Modifications in Cultured Hippocampal Neurons: Dependence on Spike Timing, Synaptic Strength, and Postsynaptic Cell Type. *J. Neurosci.* **1998**, *18*, 10464–10472.
49. Shen, K.; Meyer, T. Dynamic Control of CaMKII Translocation and Localization in Hippocampal Neurons by NMDA Receptor Stimulation. *Science* **1999**, *284*, 162–166.